Research Article

Paniz Zinsaz, Hoda Jafarizadeh-Malmiri*, Navideh Anarjan, Ali Nekoueifard, and Afshin Javadi

Effectiveness of pH and amount of *Artemia urumiana* extract on physical, chemical, and biological attributes of UV-fabricated biogold nanoparticles

https://doi.org/10.1515/gps-2022-8062
received October 28, 2022; accepted February 07, 2023

Abstract: *Artemia urumiana* extract was prepared and used in gold nanoparticles (Au NPs) synthesis via ultraviolet radiation accelerated technique. Response surface methodology was used to evaluate the effects of amount of extract (2–8 mL) and its pH (6.5–10.5) on the particle size, polydispersity index (PDI), zeta potential, and antioxidant activity of the fabricated Au NPs. Obtained results revealed that Au NPs with small particle size (61 nm) and PDI (0.387), and high zeta potential (−18.8 mV) and antioxidant activity (13.25%) were fabricated using 5.4 mL of the prepared *A. urumiana* extract with a pH value of 10.5. These optimum conditions were used in Au NPs synthesis, and NPs characteristics were assessed. Results indicated that the colloidal solution containing synthesized Au NPs had a broad emission peak at a wavelength of 562 nm. Furthermore, transmission electron microscopy analysis show that the fabricated spherical NPs had a mean particle size of 25 nm. Finally, bactericidal effects of the fabricated Au NPs were assessed against four selected bacteria strains, namely, *Staphylococcus aureus*, *Escherichia coli*, *Bacillus subtilis*, and *Pseudomonas aeruginosa*, and results indicated that synthesized NPs had strong antibacterial activity toward those, with clear zone diameters of 16, 17, 11, and 17 mm, respectively.

Keywords: *Artemia urumiana* extract, gold nanoparticles, optimization, physico-chemical properties, ultraviolet radiation

1 Introduction

Gold nanoparticles (Au NPs) have gained more interests among all other inorganic NPs because of their desirable biocompatibility, optoelectronic properties, and antimicrobial activity against various prokaryotic and eukaryotic cells. Au NPs, due to their high surface-to-volume ratio, have unique properties and high potential applications in food, biotechnology, and medicine areas [1–4]. For example, Au NPs have been broadly utilized in drug delivery and controlled release, cancer trophy, gene expression procedures, and nanobiosensors [4–6]. Moreover, Au NPs have strong antimicrobial activity toward different microorganisms such as bacteria, mold, yeast, protozoa, algae, cyanobacteria, and virus [1].

Biologically synthesized Au NPs using numerous microorganisms, enzymes, and plants, with high potential applications, have gained more attention by scientists, researchers, and manufacturers [1,2,5]. For example, our previous study indicated that *Artemia urumiana* extract was composed of high amounts of different fatty acid methyl esters, such as 9-octadecenoic acid methyl ester. These esters have high antioxidant and antimicrobial activities. Likewise, the existence of numerous carboxyl and hydroxyl functional groups in their chemical structures indicated that the extract could successfully reduce gold ions into gold elements and convert those into stable Au NPs [7]. Several studies indicated that *A. urumiana*, a brine shrimp of Urmia Lake (West Azarbaijan, Iran), has high amounts of proteins and mycosporine-like amino

* **Corresponding author: Hoda Jafarizadeh-Malmiri,** Department of Food Engineering, Faculty of Chemical Engineering, Sahand University of Technology, Tabriz, 1996-51335, Iran, e-mail: h_jafarizadeh@sut.ac.ir, tel: +98-413-3459099, fax: +98-413-3444355
Paniz Zinsaz: Department of Food Science and Technology, Mamaghan Branch, Islamic Azad University, Mamaghan, Iran
Navideh Anarjan, Afshin Javadi: Department of Food Hygiene, Faculty of Veterinary, Tabriz Medical Science, Islamic Azad University, Tabriz, Iran
Ali Nekoueifard: National Artemia Research Center, Iranian Fisheries Science Research Institute, Agricultural Research, Education and Extension Organization, Urmia, Iran

acids. Furthermore, its cyst shells are a main source of chitin, precursor of chitosan, with various amine groups (NH_3) in their chemical structures that help to synthesize more stable inorganic NPs [8–13].

Several parameters have influenced the yield of Au NPs biosynthesis process and the characteristics of the fabricated NPs, in *in vitro* studies. The concentration and the type of reducing and stabilizing components (e.g., phenols, carbohydrates, proteins, and enzymes) in the prepared natural extract, accelerated heating methods (microwave heating, hydrothermal based on autoclave, ultrasonication, and ultraviolet (UV) irradiation), and operation conditions (e.g., temperature, pressure, and pH) are the main affecting parameters in the synthesis of inorganic NPs [14–18]. Some studies revealed that changes in the pH of colloidal solutions containing gold ions and natural extract could affect the reactivity of existing reductants and stabilizers in the media, and also the coverage layer on the surface of the synthesized NPs, which alter particles size, polydispersity index (PDI), and stability (zeta potential) of the fabricated Au NPs [19–22]. Our previous study revealed that *A. urumiana* extract could easily synthesize Au NPs through six different accelerated and normal heating methods, namely, microwave, hydrothermal, UV irradiation, ultrasonication, common heating with a stirrer, and self-assembling at ambient conditions. However, UV-synthesized Au NPs had more desirable and acceptable characteristics compared to those that were fabricated by other methods [7]. Therefore, the main objectives of this study are as follows: (i) UV-assisted fabrication of Au NPs using *A. urumiana* extract, (ii) to optimize the Au NPs fabrication process parameters based on the pH value and the amount of *A. urumiana* extract in the colloidal solution containing gold ions, and (iii) to evaluate phyico-chemical characteristics and antibacterial activity of the fabricated Au NPs under optimum conditions.

2 Materials and methods

2.1 Materials

A. urumiana biomass (in the frozen state) was obtained from Artemia research center – East North Branch (Urmia, West Azarbaijan, Iran). $HAuCl_4$ having 3 H_2O, as gold salt, and 2,2-diphenyl-2-picrylhydrazyl (DPPH), as a reagent for the antioxidant test, were provided from Sigma-Aldrich (MO, USA). *Staphylococcus aureus* (PTCC 1764), *Escherichia coli* (PTCC 1270), *Bacillus subtilis* (PTCC 1023), and *Pseudomonas aeruginosa* (PTCC 1310), as main foodborne pathogens, were provided from microbial Persian type culture collection (PTCC, Tehran, Iran). Nutrient agar was purchased from Biolife (Milan, Italy). Deionized water was bought from Dr. Mojallali Chemical Complex (Tehran, Iran).

2.2 *A. urumiana* extract preparation and synthesis of Au NPs

A. urumiana extract was prepared according to the described method in our previous study, as shown in Figure 1a–f [7]. To synthesize Au NPs, based on our previous work and preliminary laboratory tests, defined amounts of the extract (2–8 mL) with different pH values (6.5–10.5) had been added into 5 mL $HAuCl_4$ solutions (1 mM), and the mixture solutions were located at 10 cm distance from UV light (365 nm), overnight. The pH of the extract was adjusted using 1 N NaOH solution.

2.3 Analyses

The pH value of the extract and sample solutions was measured by a pH meter (DELTA 320, Shanghai, China). The surface plasmon resonance (SPR) character of the synthesized Au NPs was assessed using UV-Vis spectrophotometry (Jenway UV-Vis spectrophotometer 6705, Staffordshire, UK). Particle size and particle size distribution (PSD), PDI, and zeta potential values of the fabricated Au NPs were evaluated using a dynamic light scattering particle size analyzer (Nanotrac Wave, Microtrac, USA). Morphological attributes of the formed Au NPs were observed by transmission electron microscopy (TEM; CM120, Philips, Amsterdam, the Netherlands). For the colloidal solution containing synthesized Au NPs, antioxidant activity, based on the free radical scavenging test, and antibacterial activity, based on the agar diffusion method, were accomplished [7]. Antioxidant and antibacterial activities of the samples were reported as the percentage of inhibition (% I) and diameter of a clear zone (mm), respectively. Total phenol content of the prepared extract was measured using the described method by Ghavidel et al. [23].

Figure 1: Schematic of the preparation of *A. urumiana* extract: freezed *A. urumiana* (a), freeze dryer (b), *A. urumiana* powder (c), dissolution of powder (d), filtration (e), and pH adjustment (f).

2.4 Experimental design and data analysis

Central composite design (CCD) and response surface methodology (RSM) were used to design experiments and estimate effectiveness of two selected synthesized variables including pH (X_1, 6.5–10.5) and the amount of the prepared *A. urumiana* extract (X_2, 2–8 mL) on four selected responses, namely, particle size (Y_1, nm), PDI (Y_2), Zeta potential (Y_3, mV), and antioxidant activity (Y_4, % *I*) of the prepared colloidal solutions containing formed Au NPs. As compared to other experimentation methodologies, which they are established on classical one-variable-a time optimization, RSM has several advantages [23,24]. According to the CCD, 1 block and 13 experimental runs were provided, and the center point (X_1, 8.5 and X_2, 5) was repeated five times to decrease the errors [24]. Responses (Y) were interrelated to the independent parameters by a second full quadratic equation (Eq. 1) containing linear (X_1 and X_2), quadratic (X_1^2 and X_2^2), and interaction (X_1X_2) terms, with relevant coefficients of β_0 (constant), β_1 and β_2 (linear), β_{11} and β_{22} (quadratic), and β_{12} (interaction).

$$Y = \beta_0 + \beta_1 X_1 + \beta_2 X_2 + \beta_{11} X_1^2 + \beta_{22} X_2^2 + \beta_{12} X_1 X_2 \quad (1)$$

Fitness, capability, and suitability of the resulted models were assessed through analysis of variance (ANOVA), and values for the coefficient of determination (R^2) and lack of fit (p-value) of the models were obtained. Moreover, ANOVA based on p-value less than 5% ($p < 0.05$) was utilized in significance determinations of the model terms and comparison of the obtained mean values of data (based on Tukey's comparison test) [25]. Contour and surface plots were also provided to well imagining of the effects of independent variables on the selected responses [26]. Finally, validation of the fitted models and predicted values for optimum amounts of the independent parameters were accomplished based on performing three extra tests using obtained optimal conditions [27]. CCD, RSM, optimization (including numerical and graphical), model generation, verification, and ANOVA were

completed using Minitab v.16 statistical package (Minitab Inc., PA, USA).

3 Results and discussion

3.1 Specifications of *A. urumiana*

Results of gas chromatography in our previous study indicated that fatty acids methyl esters, such as 9-octadecenoic, 11-octadecenoic, hexadecenoic, and tetradecanoic acid methyl esters, are the main bioactive compounds in the *A. urumiana* extract [7]. Furthermore, pH of the provided extract was 6.5, and its color was brown (Figure 1f). Results also indicated that the prepared extract has antioxidant activity and total phenol content of 88.7% and 810 $\mu g \cdot g^{-1}$ (based on gallic acid).

3.2 Model generation

According to the obtained values for the particle size, PDI, zeta potential, and antioxidant activity of the synthesized Au NPs (13 experimental runs in Table 1), models were generated, and the coefficients and p-values of those terms are presented in Table 2. Results revealed that the quadratic term of the prepared extract had an insignificant effect on the particle size of the fabricated NPs. Furthermore, all terms of the synthesized variables had significant ($p < 0.05$) effect on PDI of the formed Au NPs. As clearly observed in Table 2, the main and quadratic terms of pH and the prepared extract had insignificant effects on the zeta potential of the fabricated NPs. Results also demonstrated that the main term of the prepared extract and its interaction with pH had insignificant effects on the antioxidant activity of the resulted Au NPs. High R^2 values, ranging from 85.65% to 97.32%, and higher values of the lack of fit for the generated models indicated that the models had high fitness and accuracy to predict responses in the defined ranges for the synthesized parameters [28].

3.3 Effects of independent parameters on Au NPs particle size

UV irradiation is a photolysis method, which by creating the photolysis cycles can cause a loss of electrons from the metal NPs that leads to a transient state preceding the entire breakup of the larger particles [7]. Results of the experimental study indicated that the particle size of the fabricated Au NPs using different amounts of the prepared *A. urumiana* extract and different pH values varied from 39.0 to 160.5 nm (Table 1). Effects of the pH value and the amount of the prepared extract on the particle size of the synthesized Au NPs are shown in Figure 2a and b. As shown in Figure 2a, at low and constant amounts of the prepared extract, by increasing the pH of the extract, the size of NPs was constant. However, using high amounts of the prepared extract, by increasing its pH, the particle size

Table 1: CCD and values of response variables (predicted and experimental) for synthesis of Au NPs using *A. urmiana* extract

Runs	pH	Amount of extract (mL)	Particle size (nm)		PDI		Zeta potential (mV)		Antioxidant (%)	
			Exp[a]	Pre[b]	Exp[a]	Pre[b]	Exp[a]	Pre[b]	Exp[a]	Pre[b]
1	9.9	7.1	39.0	39.0	0.624	0.561	−15.0	−15.4	*	*
2	8.5	5.0	86.0	74.0	0.223	0.254	−16.9	−15.7	7.0	6.2
3	8.5	8.0	*	*	0.614	0.667	−14.9	−14.8	13.6	13.5
4	9.9	2.9	*	*	*	*	*	*	*	*
5	8.5	5.0	75.0	74.0	0.263	0.254	−15.3	−15.7	*	*
6	8.5	2.0	67.0	67.1	1.000	0.964	−16.3	−16.8	10.0	9.9
7	7.0	2.9	74.0	73.5	0.927	0.971	−14.4	−13.6	7.7	7.9
8	6.5	5.0	161.0	160.5	0.676	0.653	−14.3	−15.0	8.8	8.5
9	8.5	5.0	74.0	74.0	0.254	0.254	−15.5	−15.7	6.3	6.2
10	10.5	5.0	70.0	70.0	0.329	0.369	−19.8	−19.4	13.0	13.0
11	8.5	5.0	61.0	74.0	0.277	0.254	−15.5	−15.7	5.1	6.2
12	7.0	7.1	*	*	0.574	0.556	−16.7	−16.3	11.2	11.4
13	8.5	5.0	74.0	74.0	0.254	0.254	−15.5	−15.7	6.6	6.2

[a]Experimental values of studied responses. [b]Predicted values of studied responses. *Out of range.

Table 2: Regression coefficients and p values for the generated model terms, and R^2 and lack-off-fit's p-values of the models

Regression coefficient	Particle size (nm)	p value	PDI	p value	Zeta potential (mV)	p value	Antioxidant (%)	p value
β_0 (constant)	372.6	0.066	8.76	0.000	6.75	0.598	84.58	0.004
β_1 (main)	−122.2	0.016	−1.33	0.000	−1.93	0.476	−17.48	0.003
β_2 (main)	119.9	0.005	−0.96	0.000	−5.34	0.009	−4.12	0.084
β_{11} (quadratic)	10.3	0.005	−3.40	0.001	0.37	0.046	1.14	0.002
β_{22} (quadratic)	1.5	0.382	0.064	0.000	0.00	0.926	0.60	0.001
β_{12} (interaction)	−15.1	0.009	0.03	0.017	−0.67	0.006	−0.16	0.487
R^2 (%)	96.65		98.30		85.65		97.32	
Lack-of-fit (p-value)	>0.05		>0.05		>0.05		>0.05	

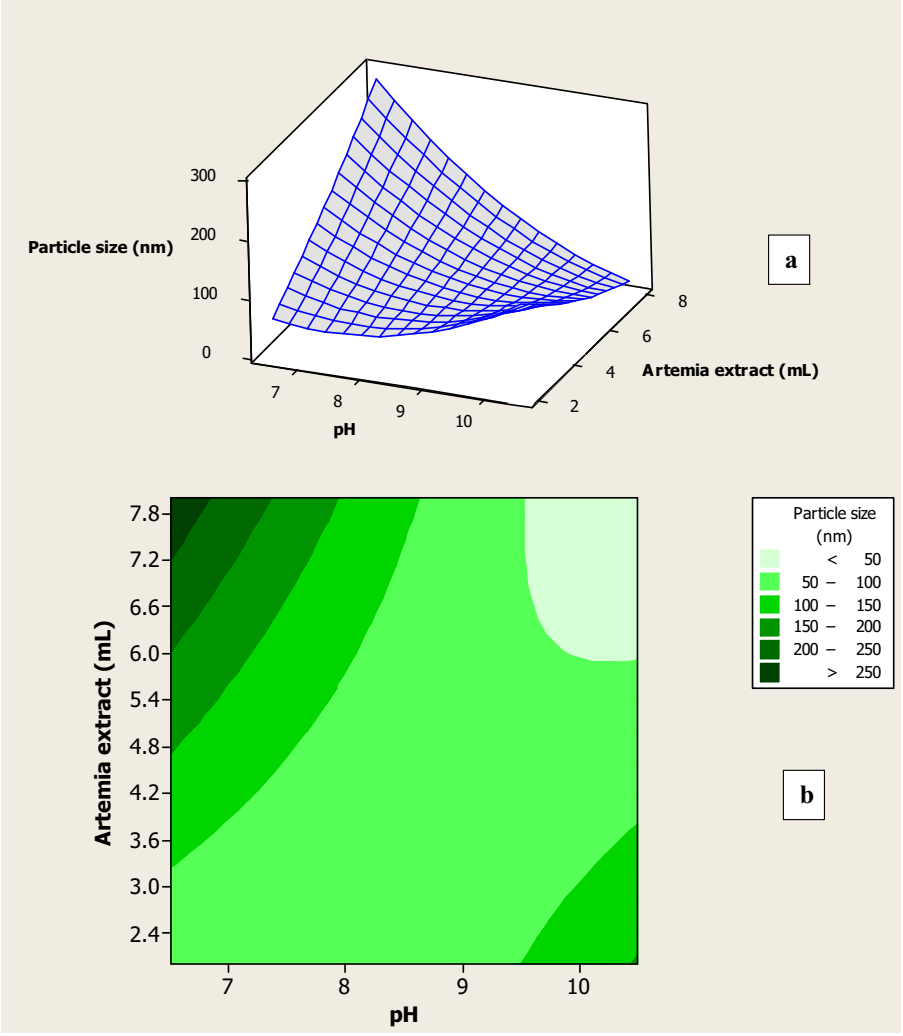

Figure 2: Surface plot (a) and contour plot (b) for particle size of the fabricated Au NPs as function of amount and pH of the prepared *A. urumiana* extract.

of the fabricated Au NPs was decreased, and these opposite trends indicated that the interaction term of the synthesized parameters had a significant effect on the particle size of the synthesized Au NPs (as its p-value of 0.009, $p < 0.05$, seen in Table 2). Figure 2b also shows that Au NPs with a small particle size were fabricated using highest amounts of the prepared extract and pH values. These results can be explained by the fact that, at high amounts of the prepared

A. urumiana extract, the concentration of bioactive compounds, which contained different fatty acid methyl esters, increases [8–10]. Furthermore, increasing the pH of the extract caused alkaline hydrolysis of these components, and various derived materials having carboxyl (COOH) and hydroxyl (OH) were formed in the colloidal solutions and could fast and easily reduce most of the gold ions and converted those into Au NPs with a small particle size. On the other hand, at high amounts of extract, the concentration of proteins and mycosporine-like amino acids, which were the main N-sources of bioactive compounds of the *A. urumiana*, were increased, and these components could easily stabilize the prepared new NPs and provided high stable synthesized Au NPs with uniform shape and size [11–13]. Obtained results were close to the findings of Eskandari-Nojedehi et al. [3]. They reported that in green synthesis of Au NPs with edible mushroom extract and using microwave heating, Au NPs with minimum particle size of 33.56 nm, were synthesized using high amounts of the extract. That was related to high concentrations of natural reducing and stabilizing bioactive compounds in the high amounts of the prepared extract.

3.4 Influences of the independent parameters on Au NPs PDI

As clearly observed in Table 1, PDI of the fabricated Au NPs in the 13 colloidal solutions changed from 0.223 to 1.000. PDI can be correlated into the PSD of the produced inorganic NPs, and its value alters from 0 to 1. In fact, small values of PDI indicate that mono-dispersed NPs, with a narrow PSD curve, are synthesized in the colloidal solution, and *vice versa* [23]. Figure 3a and b shows effectiveness of the selected parameters on PDI of the fabricated Au NPs. According to Figure 3a, at low and constant amounts of the prepared extract, by increasing the pH value of the solution, PDI of the synthesized NPs was decreased. The result can be explained by the fact that by increasing the pH of the mixture solution, the surface charge density of the formed Au NPs increases, which increases repulsion between synthesized Au NPs and the NPs in a mono-dispersed form with the minimum PDI [29,30]. At high amounts of the prepared extract, by increasing the pH value of the solution, significant changes had not been detected in the PDI of the fabricated Au NPs. In fact, the presence of curving in Figure 3a demonstrated that the interaction term of the independent variables had a significant ($p < 0.05$) effect on PDI of the synthesized NPs and reconfirmed the obtained p-value of 0.017 for this interaction term (Table 2). Figure 3b shows that the maximum PDI was obtained using minimum amounts of the prepared extract and its pH values. However, the minimum PDI for the synthesized Au NPs was obtained using amounts of the extract with it pH at the center point (pH of 8.5 with extract mount of 5.0). According to Table 1, maximum PDI was observed for the synthesized Au NPs using the minimum amount of the prepared extract, run number of 6, which can be related to the minimum concentrations of reducing and stabilizing biomaterials in the extract.

3.5 Effects of pH and provided extract on zeta potential of the synthesized Au NPs

According to Table 1, the zeta potential value of the fabricated Au NPs changes from –14.3 to –19.8 mV. The zeta potential can be correlated to the density of electric charge on the surface of NPs, and its high values indicate the formed NPs in the colloidal solutions have high stability [29,30]. The negative values of the zeta potential for the fabricated Au NPs using *A. urumiana* extract were related to the carboxylic groups in ionic form in the chemical structure of fatty acid methyl esters, and they were the main existed compounds in the *A. urumiana* extract. Figure 4a and b shows the effects of the amount and pH of the prepared *A. urumiana* extract on the zeta potential values of the formed Au NPs using the UV-accelerated synthesis technique. According to Figure 4a, at low and constant amounts of the prepared extract, by increasing its pH, the zeta potential value of the formed NPs increased. At high amounts of the prepared extract, by increasing its pH, significant changes had not been observed in the zeta potential value of the produced Au NPs. In fact, by increasing the pH, fatty acid methyl esters and proteins existed in the extract were hydrolyzed and various components having COO^- and OH^- in these structures were formed, which could reduce gold ions and formed Au NPs and cover the formed NPs with a thin layer with negative charges. In fact, compared to high amounts of the prepared extract, alkaline hydrolysis could produce highest amounts of components having carboxyl and hydroxyl, with negative charges, in those structure, when low amounts of the extract were used. The presence of curving in Figure 4a also revealed that the interaction term of the parameters had a significant ($p < 0.05$) effect on the zeta potential value of the synthesized Au NPs and reconfirmed the obtained result presented in Table 2. Figure 4b indicates that the maximum zeta potential value was obtained for the synthesized Au

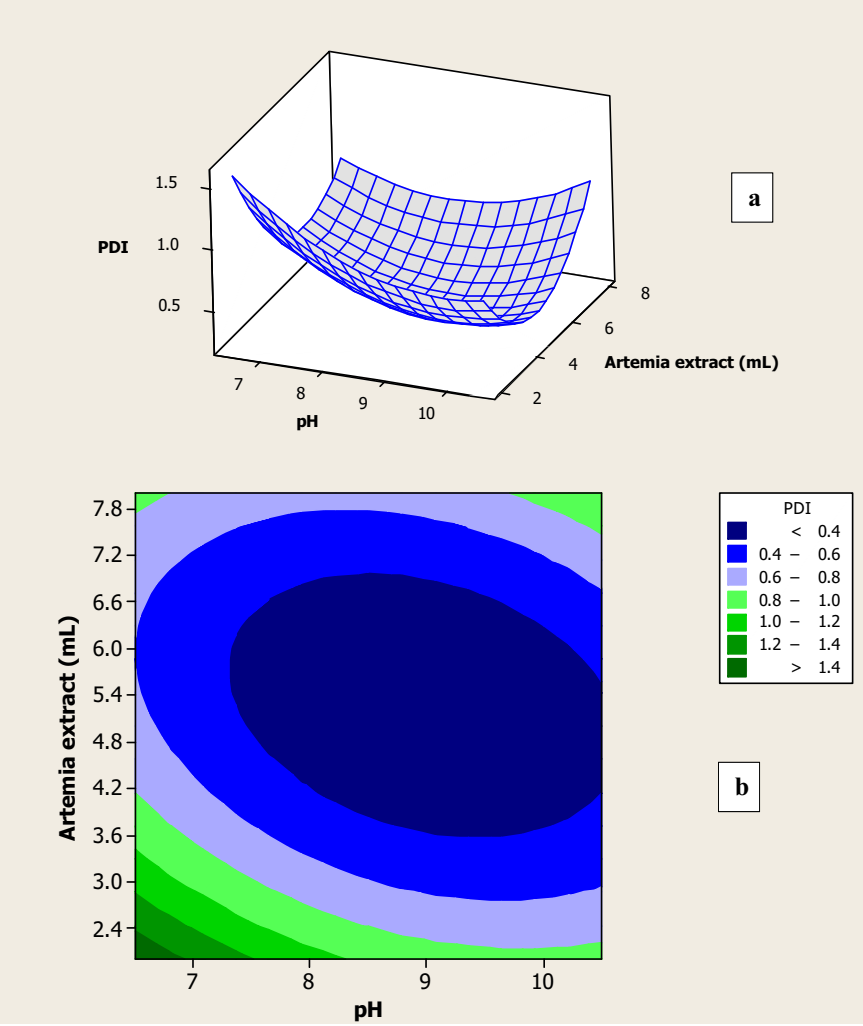

Figure 3: Surface plot (a) and contour plot (b) for PDI of the fabricated Au NPs as a function of amount and pH of the prepared *A. urumiana* extract.

NPs with low amounts of the extract and highest pH value. Table 1 also indicates that maximum zeta potential was obtained for the synthesized Au NPs using highest pH value of 10.5 (run number of 10). Rahimirad et al. hydrothermally synthesized Au NPs using four foodborne pathogens extract (*Bacillus cereus*, *E. coli*, *S. aureus*, and *Salmonella enterica* subsp. *enterica*) with zeta potential values of 15.3–30.3 mV [1]. Eskandari-Nojedehi et al. synthesized Au NPs using hydrothermally and microwave-assisted techniques and using mushroom extract with zeta potential values of 45.8 and 17.2 mV, respectively [2,3]. Eskandari-Nojedehi et al. also fabricated Au NPs with a zeta potential value of 23.4 mV using the Arabic gum and microwave heating method [4]. Abbasian and Jafarizadeh-Malmiri hydrothermally synthesized Au NPs using the coffee bean extract with a zeta potential value of 15.2 mV [5]. These indicated that the zeta potential of the fabricated Au NPs was strongly affected by the type of the extract and synthesis methods. Furthermore, several studies revealed that the synthesized metal NPs with zeta potential values of higher than +20 and lower than −20 mV have the highest stability [14–17].

3.6 Effects of the independent variables on antioxidant activity of the synthesized Au NPs

Results of experimental runs show that the antioxidant activity of the fabricated Au NPs using different amounts of the prepared *A. urumiana* extract and its different pH values varied from 5.1% to 13.6% *I* (Table 1). Furthermore, the effects of pH and the amount of prepared extract on the antioxidant activity of the fabricated NPs are shown

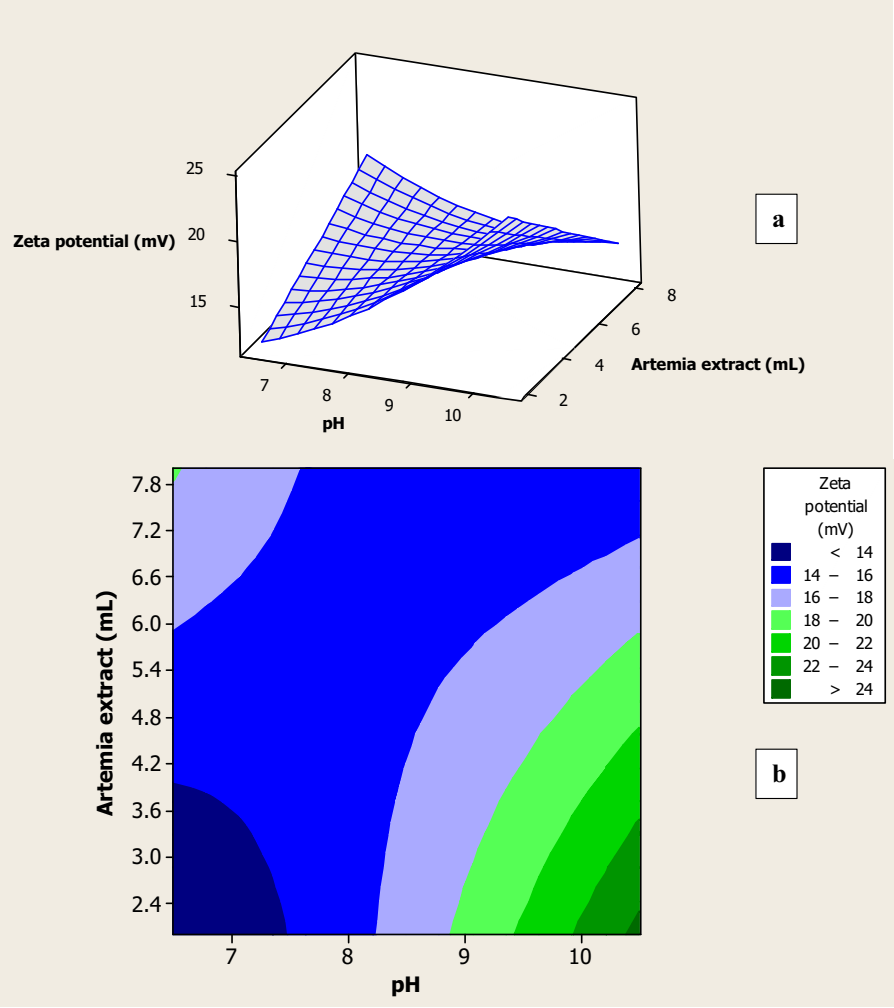

Figure 4: Surface plot (a) and contour plot (b) for zeta potential of the fabricated Au NPs as a function of amount and pH of the prepared *A. urumiana* extract.

in Figure 5a and b. As shown in Figure 5a, at any constant amounts of the prepared extract, by increasing the pH, antioxidant activity of the synthesized NPs was increased. In fact, the absence of curvature in Figure 5a indicated that the interaction term had an insignificant influence on antioxidant activity of the fabricated Au NPs. This result was in line with obtained high *p*-value of 0.487 of the interaction term, as shown in Table 2. Figure 5b also reveals that Au NPs with the highest antioxidant activity were formed using high amounts of the extract and pH values. As mentioned earlier, in the high amounts of *A. urumiana* extract, the concentration of many fatty acid methyl esters is high, and according to the previous studies, these bioactive materials have shown strong antimicrobial activity toward against numerous eukaryotic and prokaryotic cells [31,32]. Furthermore, essential fatty acids containing Omega 3 and Omega 6 have been detected in the *Artemia* extract, but the fatty acid methyl esters, especially 9-octadecenoic acid methyl ester, have highest antioxidant and anticancer activities [33,34]. This can be explicated by the fact that by decreasing the particle size of the synthesized inorganic NPs, their surface area-to-volume ratio drastically increases, which can efficiently improve and increase all characters of the resulted NPs as compared to those properties in the bulk state of inorganic materials [35]. According to Figure 2b, the minimum particle size of Au NPs was attained using highest amounts of the *A. urumiana* extract with its highest pH values.

3.7 Optimization of process and validation of the models

The numerical optimization process based on the synthesized Au NPs with small particle size and PDI, and high zeta potential and antioxidant activity, with the same

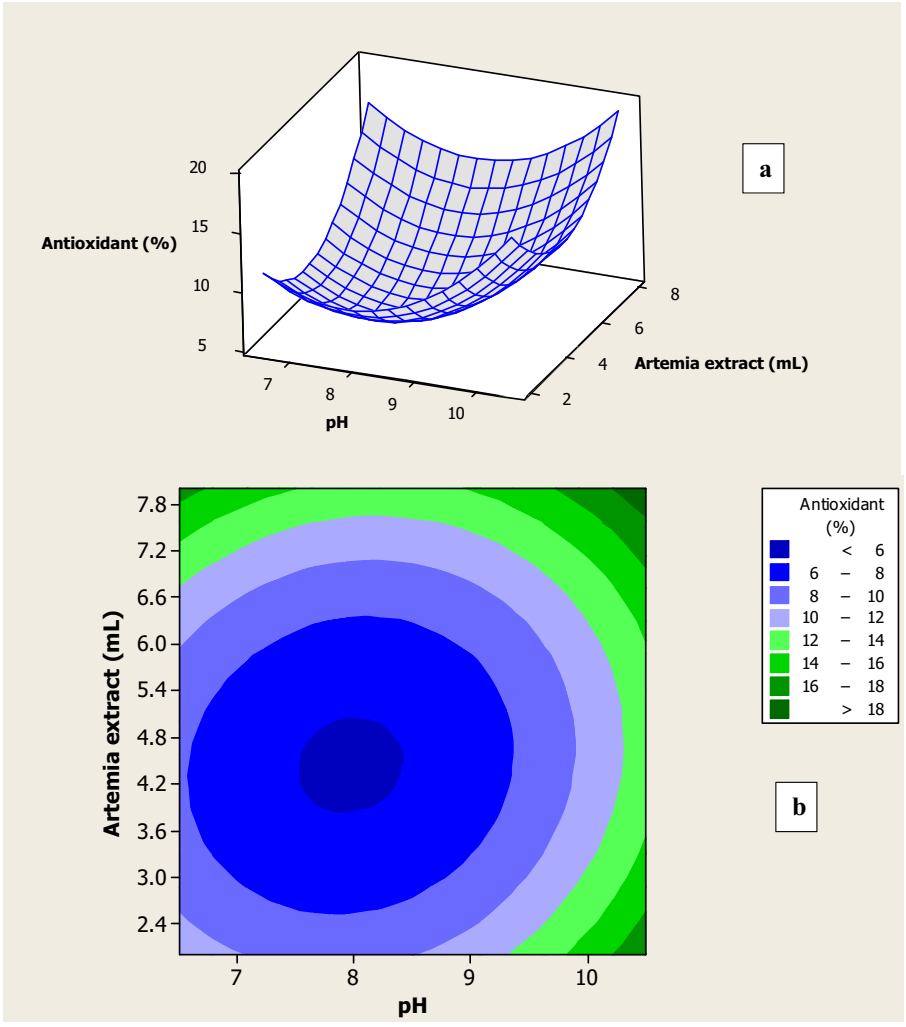

Figure 5: Surface plot (a) and contour plot (b) for antioxidant activity of the fabricated Au NPs as a function of amount and pH of the prepared *A. urumiana* extract.

importance and weight, was accomplished [36]. Results revealed that optimum conditions were attained in the fabrication of Au NPs using 5.4 mL of the prepared *A. urumiana* extract with a pH value of 10.5. By using these conditions, Au NPs had particle size, PDI, zeta potential, and antioxidant activity of 61 nm, 0.387, –18.8 mV, and 13.25% *I*, respectively. Graphical optimization, based on overlade contour plot, is shown in Figure 6. The white coloured area in this figure was related to the optimum values of the amount and pH of the prepared extract to synthesis Au NPs with more desirable responses. For verification of the suitability of the generated models by CCD and RSM, three additional experimental tests were done in the fabrication of Au NPs using predicted optimum conditions. Results demonstrated that the fabricated Au NPs had mean particle size, PDI, zeta potential, and antioxidant activity values of 63 ± 3 nm, 0.364 ± 0.025, –19 ± 0.3 mV, and 13.70 ± 0.50% *I*, respectively. The comparison test demonstrated that experimental and predicted values for the selected responses were close together, with insignificant differences, and verified the suitability and high accuracy of the fitted models [37,38].

3.8 Specifications of the fabricated Au NPs using optimal conditions

Further analyses were accomplished on the fabricated Au NPs using obtained optimum conditions. Figure 7 indicates UV-Vis spectra of the colloidal solution containing synthesized Au NPs. The presence of the broad emission peak at a wavelength of 562 nm was related to the SPR character of the Au NPs and color changes in the colloidal

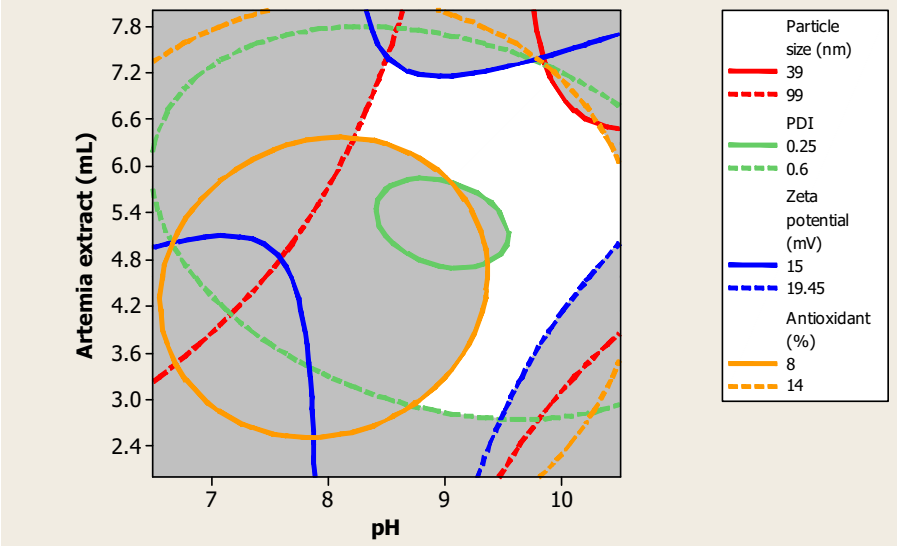

Figure 6: Overlaid contour plot of Au NPs particle size, PDI, zeta potential and antioxidant activity as a function of amount and pH of the prepared *A. urumiana* extract.

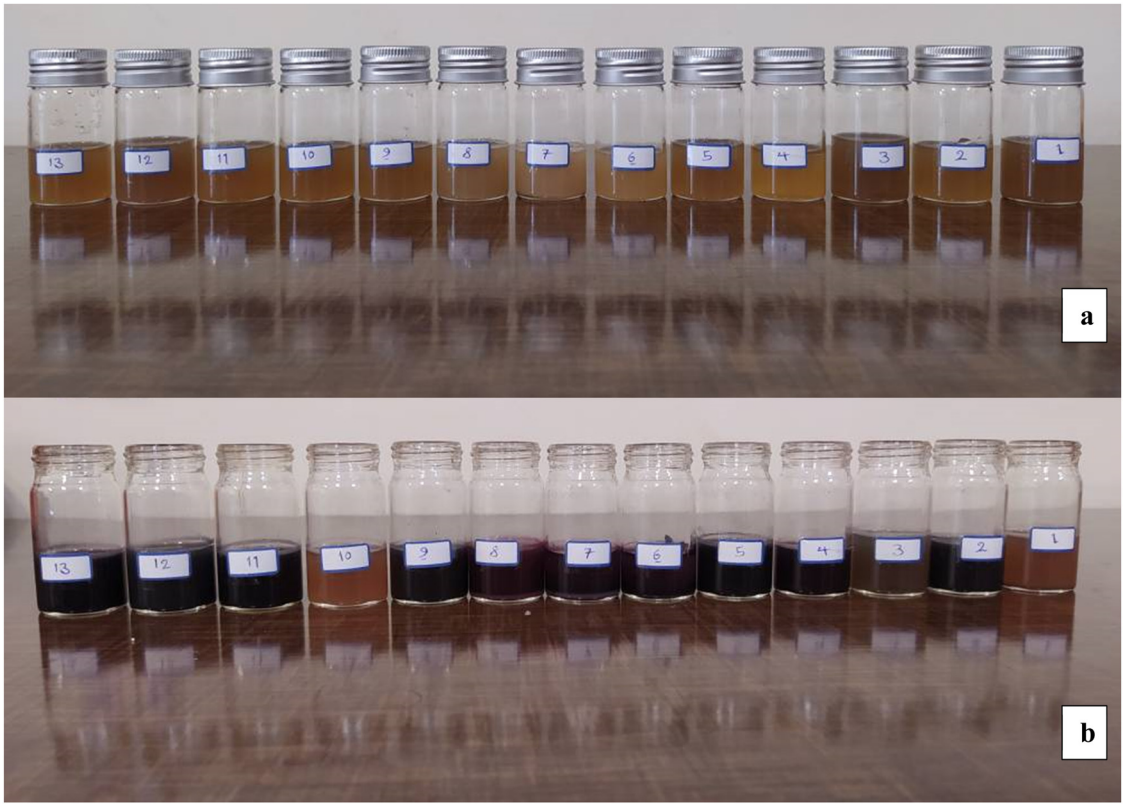

Figure 7: Appearance and color of the mixture solution before (a) and after (b) formation of the Au NPs via UV radiation.

solution before and after the formation of the NPs, which reconfirmed the formation of Au NPs using *A. urumiana* extract. Several studies indicated that the formation of Au NPs in the colloidal solutions show a broad emission peak at wavelength ranging from 510 to 570 nm, and a change in the color of the colloidal solutions into ruby [1,3,5]. Figure 8a and b shows the color of the prepared 13 colloidal solutions, according to the CCD and Table 1, before

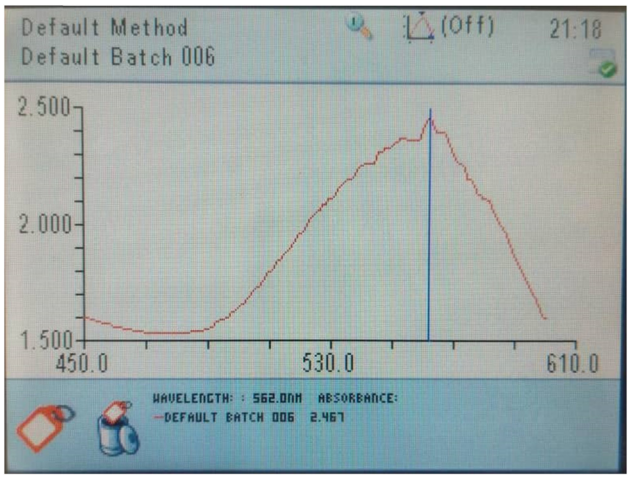

Figure 8: UV-Vis spectra of the mixture solution containing synthesized Au NPs and *A. urumiana* extract, after synthesis with UV radiation, at obtained optimum synthesis conditions.

(Figure 8a) and after (Figure 8b) exposing to the UV radiation. According to this figure, after formation of Au NPs, the color of the solutions converted from brown (Figure 8a) into ruby (Figure 8b).

The bactericidal effects of the synthesized Au NPs against four foodborne pathogenic bacteria strains were assessed, and the results indicated that the pure prepared *A. urumiana* extract did not show the bactericidal effect, and the colloidal solution containing fabricated Au NPs had high antibacterial activities toward *S. aureus*, *E. coli*, *B. subtilis*, and *P. aeruginosa* with mean clear zone diameters of 16, 17, 11, and 17 mm, respectively. Figure 9a–d shows the formed clear zones around the holes amended with the colloidal solution containing Au NPs in the plates inoculated with four different bacteria strains. Results indicated that the synthesized Au NPs had a strong bactericidal effect toward Gram-negative bacteria

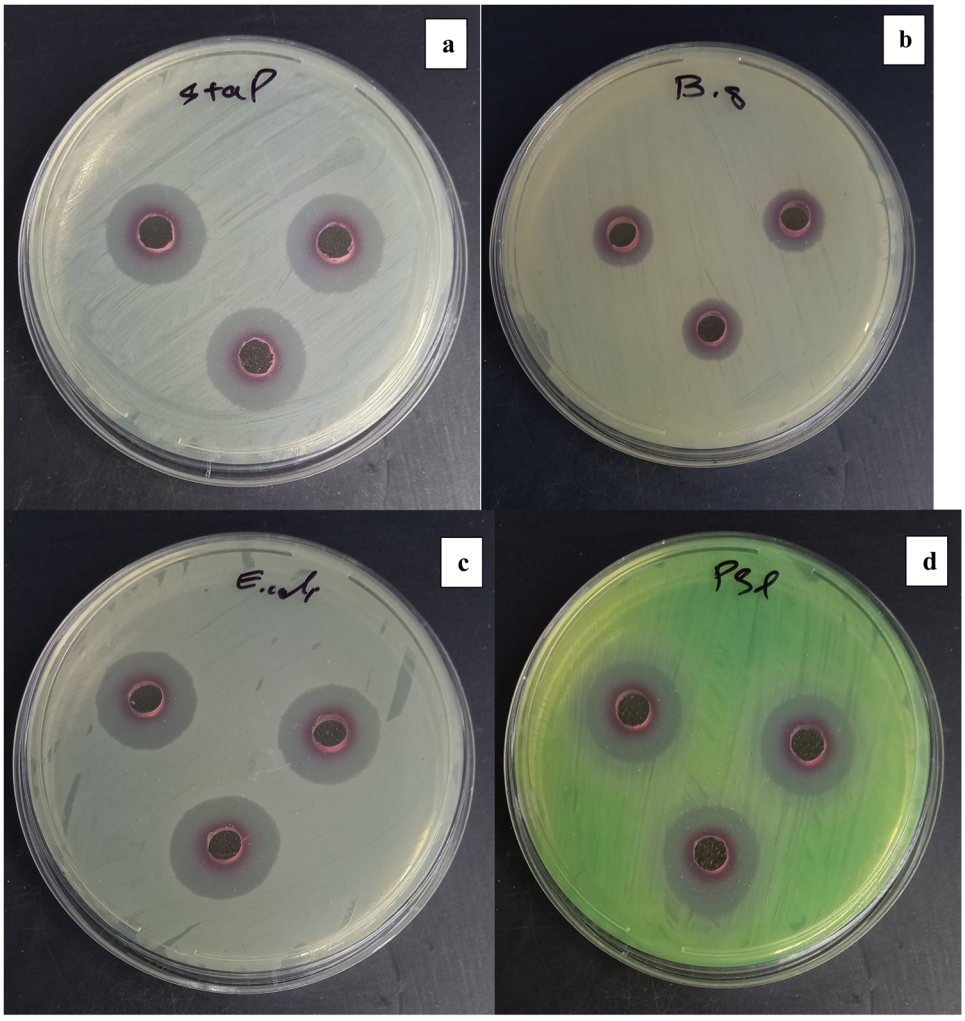

Figure 9: Bactericidal effects of the fabricated Au NPs utilizing *A. urumiana* extract and UV radiation against *S. aureus* (a), *B. subtilis* (b), *E. coli* (c), and *P. aeruginosa* (d).

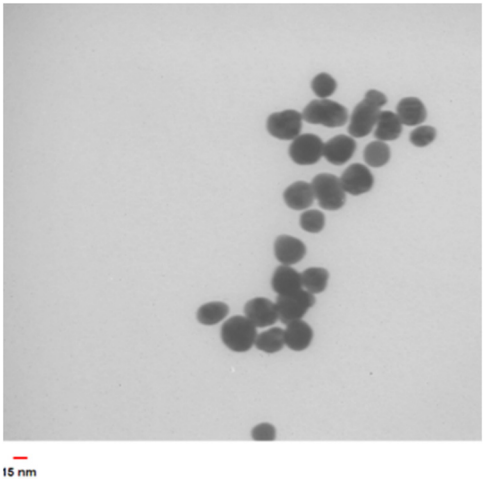

Figure 10: TEM image of the synthesized Au NPs using optimal conditions.

strains compared to Gram-positive bacteria. It seems that the main mechanism of bactericidal of the fabricated Au NPs using *A. urumiana* was related to the penetration of the formed NPs through the bacterial cell and those attachments into the cytoplasmic membrane and changing its permeability, which caused bacterial death [39]. Gram-positive bacteria strains have thicker cell walls compared to the Gram-negative bacteria, which could limit penetration of the Au NPs across that and reach the membrane [40].

Typical TEM image of the made Au NPs using UV irradiation is shown in Figure 10. As clearly observed, the spherical Au NPs with a mean particle size of 25 nm were synthesized.

4 Conclusion

In the present study, *A. urumiana* extract was prepared, and their reducing and stabilizing attributes in the reduction of gold ions and fabrication of Au NPs were evaluated. Results indicated that by using the *A. urumiana* extract with higher pH values, Au NPs with a minimum particle size and maximum stability (zeta potential value) and antioxidant activity could be easily synthesized. On the other hand, in the acidic media, Au NPs with a maximum particle size and minimum stability and antioxidant activity could be synthesized using *A. urumiana* extract with lower pH values. It also suggests that there is a need for more optimization of other synthesis parameters in the fabrication of Au NPs with the highest antioxidant and antibacterial activities for further applications in food, cosmetics, and pharmaceutics.

Acknowledgements: The authors appreciate the support of Islamic Azad University – Mamaghan branch to accomplish this research.

Funding information: The authors appreciate Islamic Azad University – Mamaghan branch for their materials, analyses, and financial supports.

Author contributions: Paniz Zinsaz: methodology, validation, investigation, resources, data curation; Hoda Jafarizadeh-Malmiri: writing – final manuscript, writing – review and editing, supervision, project administration; Navideh Anarjan: formal and data statistical analyses, writing – original draft; Ali Nekoueifard: visualization, writing – review and editing; Afshin Javadi: design of experiments, antibacterial activity assay.

Conflict of interest: The authors state no conflict of interest.

Data availability statement: All data generated or analyzed during this study are included in this published article.

References

[1] Rahimirad A, Javadi A, Mirzaei H, Anarjan N, Jafarizadeh-Malmiri H. Biological approach in nanobiotechnology–screening of four food pathogenic bacteria extract ability in extracellular biosynthesis of gold nanoparticles. Biologia. 2020;75:619–25.

[2] Eskandari-Nojedehi M, Jafarizadeh-Malmiri H, Rahbar-Shahrouzi J. Hydrothermal biosynthesis of gold nanoparticle using mushroom (*Agaricus bisporous*) extract: Physico-chemical characteristics and antifungal activity studies. Green Process Synth. 2018;7:38–47.

[3] Eskandari-Nojedehi M, Jafarizadeh-Malmiri H, Rahbar-Shahrouzi J. Optimization of processing parameters in green synthesis of gold nanoparticles using microwave and edible mushroom (*Agaricus bisporus*) extract and evaluation of their antibacterial activity. Nanotechnol Rev. 2016;5:537–48.

[4] Eskandari-Nojedehi M, Jafarizadeh-Malmiri H, Jafarizad A. Microwave accelerated green synthesis of gold nanoparticles using gum arabic and their physico-chemical properties assessments. Z Phys Chem. 2018;232:325–43.

[5] Abbasian R, Jafarizadeh-Malmiri H. Green approach in gold, silver and selenium nanoparticles using coffee bean extract. Open Agric. 2020;5:761–7.

[6] Kumar B, Smita K, Sánchez E, Guerra S, Cumbal L. Ecofriendly ultrasound-assisted rapid synthesis of gold nanoparticles using Calothrix algae. Adv Nat Sci: Nanosci Nanotechnol. 2016;7(2):025013.

[7] Zinsaz P, Jafarizadeh-Malmiri H, Anarjan N, Nekoueifard A, Javadi A. Biogenic synthesis of gold nanoparticles using *Artemia urumiana* extract and five different thermal accelerated techniques: Fabrication and characterization. Z Naturforsch C. 2022;77(9–10):395–402.
[8] Deezagi A, Chashnidel A, Hagh NV, Shahraki MK. The effects of purified *Artemia* extract proteins on proliferation, differentiation and apoptosis of human leukemic HL-60 cells. Asian Pac J Cancer Prev. 2016;17(12):5139–45.
[9] Abatzopoulos TJ, Baxevanis AD, Triantaphyllidis GV, Criel G, Pador EL, Van Stappen G, et al. Quality evaluation of *Artemia urumiana* Günther (Urmia Lake, Iran) with special emphasis on its particular cyst characteristics (International Study on Artemia LXIX). Aquac. 2006;254(1–4):442–54.
[10] Khosravi S, Khodabandeh S, Agh N, Bakhtiarian M. Effects of salinity and ultraviolet radiation on the bioaccumulation of mycosporine-like amino acids in artemia from lake urmia (Iran). Photochem Photobiol. 2013;89(2):400–5.
[11] Asem A, Mohebbi F, Ahmadi R. Drought in Urmia Lake, the largest natural habitat of brine shrimp Artemia. World Aquaculture. 2012;43(1):36–8.
[12] Vaseli-Hagh N, Deezagi A, Shahraki MK. Anti-aging effects of the proteins from Artemia extract on human fibroblasts cell proliferation and collagen expression in induced aging conditions. Ann Biotechnol. 2018;3:1–7.
[13] Tajik H, Moradi M, Rohani SMR, Erfani AM, Jalali FSS. Preparation of chitosan from brine shrimp (Artemia urumiana) cyst shells and effects of different chemical processing sequences on the physicochemical and functional properties of the product. Molecules. 2008;13(6):1263–74.
[14] Torabfam M, Jafarizadeh-Malmiri H. Microwave – enhanced silver nanoparticles synthesis using chitosan biopolymer – Optimization of the process conditions and evaluation of their characteristics. Green Process Synth. 2018;7:530–7.
[15] Mohammadlou M, Jafarizadeh-Malmiri H, Maghsoudi H. A review on green silver nanoparticles based on plants: synthesis, potential applications and eco-friendly approach. Int Food Res J. 2016;23:446–63.
[16] Ahmadi O, Jafarizadeh-Malmiri H, Jodeiri N. Eco-friendly microwave enhanced green silver nanoparticles synthesis using *Aloe vera* Leaf extract and their physico-chemical and antibacterial studies. Green Process Synth. 2018;7:231–40.
[17] Fardsadegh B, Jafarizadeh-Malmiri H. Aloe vera leaf extract mediated green synthesis of selenium nanoparticles and assessment of their *in vitro* antimicrobial activity against spoilage fungi and pathogenic bacteria strains. Green Process Synth. 2019;8(1):399–407.
[18] Vahidi A, Vaghari H, Najian Y, Najian MJ, Jafarizadeh-Malmiri H. Evaluation of three different green fabrication methods for the synthesis of crystalline ZnO nanoparticles using Pelargonium zonale leaf extract. Green Process Synth. 2019;8:302–8.
[19] Yazdani S, Daneshkhah A, Diwate A, Patel H, Smith J, Reul O, et al. Model for gold nanoparticle synthesis: Effect of pH and reaction time. ACS Omega. 2021;6(26):16847–53.
[20] Dubey SP, Lahtinen M, Sillanpää M. Tansy fruit mediated greener synthesis of silver and gold nanoparticles. Process Biochem. 2010;45(7):1065–71.
[21] Annur S, Santosa SJ, Aprilita NH. pH dependence of size control in gold nanoparticles synthesized at room temperature. Orient J Chem. 2018;34(5):2305–12.
[22] Zhu J, Li W, Zhu M, Zhang W, Niu W, Liu G. Influence of the pH value of a colloidal gold solution on the absorption spectra of an LSPR-assisted sensor. AIP Adv. 2014;4(3):031338. doi: 10.1063/1.4869615.
[23] Ghavidel F, Javadi A, Anarjan N, Jafarizadeh-Malmiri H. New approach in process intensification based on subcritical water, as green solvent, in propolis oil in water nanoemulsion preparation. Green Process Synth. 2021;10(1):208–18.
[24] Ahdno H, Jafarizadeh-Malmiri H. Development of a sequenced enzymatically pre-treatment and filter pre-coating process to clarify date syrup. Food Bioprod Process. 2017;101:193–204.
[25] Faramarzi S, Anzabi Y, Jafarizadeh-Malmiri H. Selenium supplementation during fermentation with sugar beet molasses and Saccharomyces cerevisiae to increase bioethanol production. Green Process Synth. 2019;8(1):622–8.
[26] Fardsadegh B, Vaghari H, Mohammad-Jafari R, Najian Y, Jafarizadeh-Malmiri H. Biosynthesis, characterization and antimicrobial activities assessment of fabricated selenium nanoparticles using Pelargonium zonale leaf extract. Green Process Synth. 2019;8(1):191–8.
[27] Yari T, Vaghari H, Adibpour M, Jafarizadeh-Malmiri H, Berenjian A. Potential application of Aspergillus terreus, as a biofactory, in extracellular fabrication of silver nanoparticles. Fuel. 2022;308:122007. doi: 10.1016/j.fuel.2021.122007.
[28] Mohammadlou M, Jafarizadeh-Malmiri H, Maghsoudi H. Hydrothermal green silver nanoparticles synthesis using *Pelargonium/Geranium* leaf extract and evaluation of their antifungal activity. Green Process Synth. 2017;6:31–42.
[29] Pourali P, Benada O, Pátek M, Neuhöferová E, Dzmitruk V, Benson V. Response of biological gold nanoparticles to different pH values: Is It possible to prepare both negatively and positively charged nanoparticles? Appl Sci. 2021;11(23):11559. doi: 10.3390/app112311559.
[30] Ghanbari S, Vaghari H, Sayyar Z, Adibpour M, Jafarizadeh-Malmiri H. Autoclave-assisted green synthesis of silver nanoparticles using A. fumigatus mycelia extract and the evaluation of their physico-chemical properties and antibacterial activity. Green Process Synth. 2018;7(3):217–24.
[31] Hatami R, Javadi A, Jafarizadeh-Malmiri H. Effectiveness of six different methods in green synthesis of selenium nanoparticles using propolis extract: Screening and characterization. Green Process Synth. 2020;9(1):685–92.
[32] Chandrasekaran M, Kannathasan K, Venkatesalu V. Antimicrobial activity of fatty acid methyl esters of some members of Chenopodiaceae. Z Naturforsch C J Biosci. 2008;63(5–6):331–6.
[33] Asghar SF, Choudahry MI. Gas chromatography-mass spectrometry (GC-MS) analysis of petroleum ether extract (oil) and bio-assays of crude extract of *Iris germanica*. Int J Genet Mol Biol. 2011;3(7):95–100.
[34] Islam SU, Ahmed MB, Shehzad A, Lee YS. Methanolic extract of *Artemia salina* eggs and various fractions in different solvents contain potent compounds that decrease cell viability of colon and skin cancer cell lines and show antibacterial activity against *Pseudomonas aeruginosa*. Evid Based Complement Altern Med. 2019;6:9528256. doi: 10.1155/2019/9528256.
[35] Soltani-Horand P, Vaghari H, Soltani-Horand J, Adibpour M, Jafarizadeh-Malmiri H. Extracellular mycosynthesis of antibacterial silver nanoparticles using *Aspergillus flavus* and evaluation of their characteristics. Int J Nanosci. 2020;19(2):1950009. doi: 10.1142/S0219581X19500091.

[36] Rahimirad A, Javadi A, Mirzaei H, Anarjan N, Jafarizadeh-Malmiri H. Biosynthetic potential assessment of four food pathogenic bacteria in hydrothermally silver nanoparticles fabrication. Green Process Synth. 2019;8(1):629–34.
[37] Ahmadi O, Jafarizadeh-Malmiri H. Intensification process in thyme essential oil nanoemulsion preparation based on sub-critical water as green solvent and six different emulsifiers. Green Process Synth. 2021;10(1):430–9.
[38] Anvarinezhad M, Javadi A, Jafarizadeh-Malmiri H. Green approach in fabrication of photocatalytic, antimicrobial, and antioxidant zinc oxide nanoparticles–hydrothermal synthesis using clove hydroalcoholic extract and optimization of the process. Green Process Synth. 2020;9(1):375–85.
[39] Kon K, Rai M. Metallic nanoparticles: mechanism of antibacterial action and influencing factors. J Comp Clin Pathol Res. 2013;2:160–74.
[40] Zhou Y, Kong Y, Kundu S, Cirillo JD, Liang H. Antibacterial activities of gold and silver nanoparticles against Escherichia coli and bacillus Calmette-Guérin. J Nanobiotechnol. 2012;10:19–28.